RSC Advances

ROYAL SOCIETY OF CHEMISTRY

www.rsc.org/advances

Density Functional Theory Study on the Reaction of Triazol-3-one with Nitronium: Direct Nitration versus Acidic Group-Induced Nitration

Kuan Wang, Jian-Gang Chen, Bozhou Wang, Fengyi Liu, Zhao-Tie Liu, Zhong-Wen Liu, Wenliang Wang, Jinqiang Jiang, Zhengping Hao, Jian Lu**

Herein, an unexpected induction effect derived from the coexisted acid group (NO_3^- and/or HSO_4^-) was proposed. The impact of the induction effect and the resulted enhanced catalytic effect on the nitration of TO was systematically demonstrated.

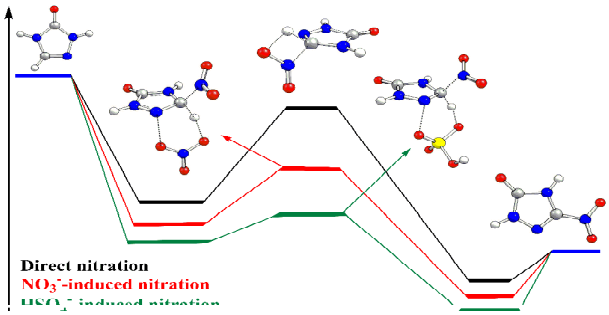

Cite this: DOI: 10.1039/c0xx00000x

www.rsc.org/xxxxxx

ARTICLE TYPE

Density Functional Theory Study on the Reaction of Triazol-3-one with Nitronium: Direct Nitration versus Acidic Group-Induced Nitration

Kuan Wang,[a] Jian-Gang Chen,*[a] Bozhou Wang,[c] Fengyi Liu,[a] Zhao-Tie Liu,[a] Zhong-Wen Liu,[a] Wenliang Wang,[a] Jinqiang Jiang,[a] Zhengping Hao[b] and Jian Lu*[c]

Received (in XXX, XXX) Xth XXXXXXXXX 20XX, Accepted Xth XXXXXXXXX 20XX
DOI: 10.1039/b000000x

The nitration mechanism as well as kinetics of triazol-3-one (TO) with nitronium (NO_2^+) in both a concentrated nitric acid and a nitric-sulfuric acids system was theoretically studied. Firstly, the density functional theory (DFT) with B3LYP functional was employed to investigate the mechanism of the mentioned reactants to the targeted product, 5-nitro-2,4-dihydro-1,2,4-triazol-3-one (NTO). An unexpected induction effect, which derived from the coexisted acid group (NO_3^- and/or HSO_4^-), was proclaimed. And the impact of the induction effect on the nitration of TO was systematically demonstrated. It is found that unlike the nitration of most aromatics, the nitration of TO with NO_2^+ to form NTO does not follow the typical electrophilic substitution mechanism. Based on the results calculated in each acid system, the nitration mechanisms, including the NO_2^+ direct nitration (path A), NO_3^--induced nitration (paths Bn-Dn) and HSO_4^--induced nitration (paths Bs-Ds), were proposed. It is indicated that the path A is unlikely or unfavorable due to the high activation barrier in the rate-determining step, whereas paths Bn-Dn and Bs-Ds are favorable, mainly attributing to the significant decrease of the activation energy induced by NO_3^- and HSO_4^- during the nitration process, especially for the NTO-oriented path Bn and Bs. Secondly, the canonical variational transition (CVT) state theory with small curvature tunneling (SCT) correction was used and the rate constants of the rate-determining steps for all paths at different temperatures were calculated. It is shown that the nitration rate in either path Bn or path Bs outdistances that in path A, indicating that NO_3^- and HSO_4^- accelerate the nitration of TO with NO_2^+, and ultimately favour the formation of NTO due to the proposed induction effect of each acid group. An enhanced catalytic effect of the nitric acid or/and sulfuric acid is thought to be embodied in not only the acceleration to the formation of NO_2^+, but also the induction effects of NO_3^- and HSO_4^- during the nitration processes. Meanwhile, it is suggested that the concentration of nitric acid and sulfuric acid in each nitration system should be well controlled since the favourable condition to produce NO_2^+ and NO_3^- /HSO_4^- differs in the concentrations of the corresponding acids.

1. Introduction

5-Nitro-2,4-dihydro-1,2,4-triazol-3-one (NTO) has been well-known as a potential high-performance insensitive energetic material since it was developed at Los Alamos National Laboratory in 1983[1]. NTO was found to have high energy release on decomposition and high detonation velocity. It was also found to have other desirable properties, including good thermal stability[2], regular crystalline structure[3], low chemical sensitivity to radiation damage[4], relatively low shock sensitivity, and low sensitivity against impact-induced ignition[5,6].

Although NTO has been studied extensively and its decomposition mechanism has attracted much attention from both experimentalists[7-11] and theoreticians[12-17], its synthesis mechanism and kinetic have been seldom investigated. So far there is no consensus on the synthesis mechanism and kinetics. NTO can be easily synthesized by the nitration of TO in a dilute/concentrated nitric acid[18], or in a nitric-sulfuric acids[19]. Zbarsky et al.[20] investigated the nitration kinetics of TO in 70-100% nitric acid experimentally. It was shown that the concentration of the nitric acid used plays an extremely important role during the nitration of TO in a concentrated nitric acid system. Cheng et al.[21] proposed the nitration mechanism of TO in nitric acid and dinitrogen pentoxide (N_2O_5), which were used as the nitration reagents. Nevertheless, the nitration mechanism of TO in concentrated nitric acid or in nitric-sulfuric acids has never been reported so far. Klapoetke et al.[22] suggested that NO_2^+ may be the nitration reagent in concentrated nitric acid and nitric-sulfuric acids system, in which the formation of NO_2^+ was also studied.[23-28] Since nitric acid and nitric-sulfuric acids are mostly

used in the nitration of TO, the nitration systems of the above mentioned acids are selected in our study so as to understand the nitration mechanism(s) of TO with NO_2^+ and to improve the further applications of the nitration systems.

The nitration reaction is known as an important method to prepare energetic materials. Most nitration processes to prepare energetic materials are found to correspond to the electrophilic substitution mechanisms, particularly in the nitration of the aromatics[29-33]. However, it seems that the nitration mechanism of TO with NO_2^+ differs dramatically in that of the aromatics, since no expected structure in which the NO_2^+ directly attached to the target C1 atom in TO could been obtained without any co-action or assist with other atom(s) or group(s) in our B3LYP/6-311G(d,p) calculations[34], as is shown in Fig. S1 in the Electronic Supplementary Information. When the NO_2^+ attacked TO, the NO_2^+ was apt to be attracted by the N8 atom instead of the C1 atom (due to the co-action of relatively low steric hindrance and relatively high electronegativity of N8, thus the NO_2^+ cannot be directly added to the C1 atom, shown in Fig. S1). The absence of a detailed synthesis mechanism of NTO hinders its further study and application to a large extent.

In the present paper, the nitration of TO with NO_2^+ in both a concentrated nitric acid and a nitric-sulfuric acids system was studied by employing the DFT with the B3LYP functional. The detailed nitration mechanism and kinetics were specially investigated. The present paper is expected to provide a better understanding of the nitration mechanism of TO with NO_2^+ under different conditions, and contribute to the optimization of the reaction conditions.

2. Computational Details

All calculations have been performed using the Gaussian 09 software package[35]. The geometries of reactant complexes, transition states, and products were optimized using DFT-B3LYP method in conjugation with the 6-311G(d,p) basis set[36,37], which has been widely used of in the similar system[21,38-40]. At the same level of theory, vibrational frequencies were calculated on all the obtained structures to verify whether they are transition structures or local minima, to provide the zero-point vibrational energy (ZPE) and to determine the thermodynamic contributions to the enthalpy and free energy. Moreover, intrinsic reaction coordinate (IRC)[41] analysis was carried out for each transition state so as to ensure that the desired reactant and product are connected to the transition structure obtained. In order to obtain more accurate relative energies, the single-point energies of all stationary points were further calculated at the B3LYP/6-3111++G(3df,3pd)//B3LYP/6-311G(d,p) level. The zero-point energies, relative energies, enthalpies, and free energies for the nitration of TO with NO_2^+ in a concentrated nitric acid and a nitric-sulfuric acids are shown in Table 1.

To investigate the rate-determining step of every nitration reaction channel without and with NO_3^- or HSO_4^-, the theoretical rate constants at different temperatures were calculated by using canonical variational transition (CVT) state theory[42-44] with small curvature tunneling (SCT) correction[45,46] in the VKLab program[47] coupled with steady state approximation. The kinetic properties of the system were calculated using conventional transition state theory (TST), the reaction starts with the formation of an intermediate before the transition states and releases the products. The energies obtained at the B3LYP/6-311++G(3df,3pd)// B3LYP/6-311G(d,p) level, and other parameters computed at the B3LYP/6-311G(d,p) level, respectively, were used in the calculations of kinetic properties.

3. Results and Discussions

3.1 Mechanism for the nitration of TO

NTO was mostly synthesized via the nitration of TO in concentrated nitric acid or nitric-sulfuric acids. It was reported that NO_2^+ may actually act as the nitration reagent in the nitration systems. The formation of NO_2^+ was as follows: after the nitric acid was protonated in concentrated acids, the protonated nitric acid ($H_2NO_3^+$) formed and might formed and might act as the

Table 1 Zero-point energies (ZPE, kcal mol^{-1}), relative energies (ΔE and ZPE (ΔE+ZPE), kcal mol^{-1}), enthalpies (ΔH(298 K), kcal mol^{-1}), and free energies (ΔG(298 K), kcal mol^{-1}) for the nitration of TO with NO_2^+ in a concentrated nitric acid or a nitric-sulfuric acids[a].

System	ZPE	ΔE	(ΔE+ZPE)	ΔG(298)	ΔH(298)
direct path					
TO + NO_2^+	47.7	0.0	0.0	0.0	0.0
A-IM1	48.6	-37.1	-32.3	-26.8	-36.5
A1-TS1	45.7	9.0	9.3	17.1	6.3
A2-TS1	45.6	12.8	13.4	20.9	10.0
A1-IM2	48.5	-45.8	-43.0	-34.7	-45.7
A1-TS2	46.3	-25.7	-25.2	-16.7	-27.9
A-IM3	49.1	-43.6	-40.2	-31.8	-42.9
NO_3^--induced path					
TO + NO_2^+ + NO_3^-	56.6	0.0	0.0	0.0	0.0
Bn-IM1	59.4	-161.4	-148.2	-137.6	-159.2
Bn-TS1	57.4	-153.4	-139.8	-130.8	-153.3
Bn-IM2	59.4	-206.8	-194.0	-183.6	-204.2
P + HNO_3	58.4	-196.1	-185.3	-184.2	-194.9
Cn-IM1	58.3	-175.1	-160.6	-153.7	-173.2
Cn-TS1	54.3	-144.3	-129.7	-126.1	-146.5
Cn-IM2	59.0	-187.1	-173.2	-164.1	-184.9
P1 + HNO_3	57.9	-176.0	-163.9	-164.8	-175.2
Dn-IM1	58.2	-174.2	-159.8	-153.1	-172.4
Dn-TS1	54.8	-145.8	-131.8	-126.9	-147.7
Dn-IM2	58.2	-178.5	-164.9	-157.7	-176.6
P2 + HNO_3	57.8	-176.4	-164.3	-165.3	-175.6
HSO_4^--induced path					
TO + NO_2^+ + HSO_4^-	64.2	0.0	0.0	0.0	0.0
Bs-IM1	66.8	-142.0	-133.9	-131.3	-140.1
Bs-TS1	65.3	-139.5	-132.4	-131.4	-139.4
Bs-IM2	66.8	-189.8	-183.3	-180.7	-187.6
P + H_2SO_4	65.6	-176.2	-172.1	-170.7	-175.3
Cs-IM1	66.2	-158.1	-149.9	-147.9	-156.1
Cs-TS1	63.1	-138.8	-130.9	-132.0	-140.3
Cs-IM2	66.5	-170.6	-163.5	-161.2	-168.7
P1 + H_2SO_4	65.1	-156.1	-150.7	-149.8	-155.7
Ds-IM1	66.2	-163.6	-154.9	-153.0	-161.9
Ds-TS1	63.5	-133.5	-125.8	-126.6	-134.5
Ds-IM2	65.8	-160.9	-154.4	-152.9	-159.3
P2 + H_2SO_4	65.1	-156.4	-151.1	-150.2	-156.0

[a] ZPE was obtained at the B3LYP/6-311G(d,p) level. The energy value was obtained at the B3LYP/6-311++G(3df,3pd) level, whereas the H and G corrections were taken from the B3LYP/6-311G(d,p) value.

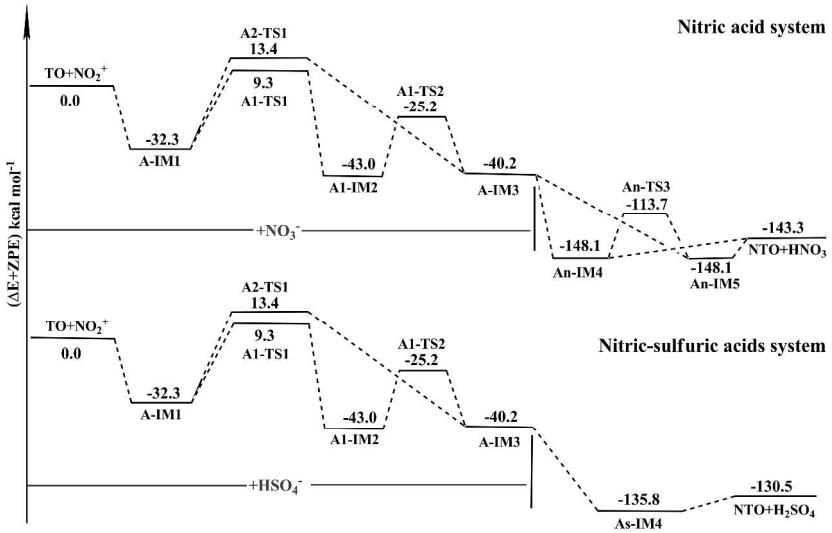

Fig. 1 Schematic energy diagram for potential energy surface of the direct nitration of TO in a concentrated nitric acid or a nitric-sulfuric acids predicted at the B3LYP/6-311++G(3df,3pd)//B3LYP/6-311G(d,p) level. Actually, NO_3^- as well as HSO_4^- did not participate in the nitration process in each pathway up to A-IM3. Here, NO_3^- and HSO_4^- were added into each pathway prior to A-IM3 only to keep the atomic conservation of nitration system.

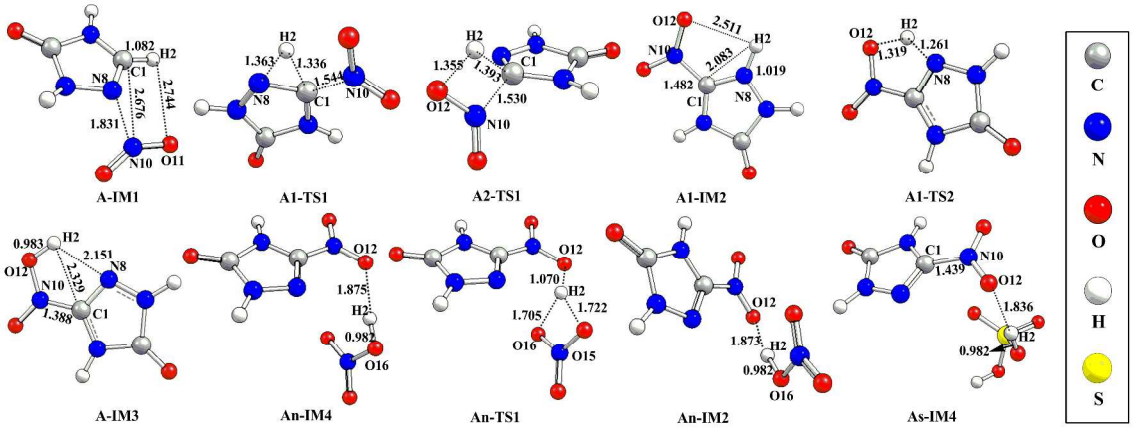

Fig. 2 Optimized geometries of species in the direct nitration of TO in a concentrated nitric acid or a nitric-sulfuric acids at the B3LYP/6-311G(d,p) level (bond lengths are in angstrom).

source of NO_2^+ by the dehydration of $H_2NO_3^+$ in the presence of a strong acid[23-28]. On the bases of CCSD(T) calculation with relatively large basis sets, Lee[48] investigated protonated forms of $H_2NO_3^+$ and found that the lowest energy form of $H_2NO_3^+$ corresponds to a complex between H_2O and NO_2^+. This complex can be easily dehydrated to form NO_2^+ in the presence of concentrated acid. Based on the literatures mentioned above, the overall reaction processes for the formation of NO_2^+ in concentrated nitric acid and in nitric-sulfuric acids may be expressed as (1) and (2), respectively.

$$HNO_3 + 2HNO_3 \rightarrow 2NO_3^- + NO_2^+ + H_3O^+ \quad (1)$$

$$HNO_3 + 2H_2SO_4 \rightarrow 2HSO_4^- + NO_2^+ + H_3O^+ \quad (2)$$

Meanwhile, NO_2^+ is found to be a more efficient nitration reagent and a better electrophile than the HNO_3 molecule. Based on such investigations, the nitration of TO in concentrated acids systems is simplified as that of TO and NO_2^+ with/without the assist of NO_3^-/HSO_4^- in the present paper.

3.1.1 NO_2^+ direct nitration mechanism

It has been reported that the most common mechanism of nitration reaction for aromatics is electrophilic substitution[29-33]. According to this theory, it is assumed that the TO nitration mechanism can be divided into two steps. Firstly, the NO_2^+ is added to the target C1 atom and formed C^+. Secondly, H atom leaves from C1 atom. However, in our B3LYP/6-311G(d,p) calculations[34], no expected structure in which the NO_2^+ directly attached to the target C1 atom has been obtained. Therefore, the above-mentioned NO_2^+ direct nitration mechanism is not supported. Instead, by further considering the possible hydrogen transfer process, two reaction paths in concentrated nitric acids or nitric-sulfuric acids are proposed and verified via employing the quantum chemical calculations. A schematic energy diagram for the NO_2^+ direct nitration reaction has been computed at the B3LYP/6-311++G(3df,3pd)//B3LYP/6-311G(d,p) level (shown

in Fig. 1). The geometrical parameters of the reactants, transition states, intermediates, and products in two reaction pathways in concentrated nitric acids and nitric-sulfuric acids are shown in Fig. 2.

As shown in Fig.1, the NO_2^+ direct nitration mechanism has two possible pathways (path A1 and A2, which pass through the transition states of A1-TS1 and A2-TS1, respectively). Started from NO_2^+ and TO, the same intermediate (A-IM3) can be obtained in both paths in the two acidic systems. Actually, mechanisms of the two acidic systems are roughly the same before the formation of A-IM3.

Firstly, TO and NO_2^+ form an intermediate IM1, which is found in a deep potential well of -32.3 kcal mol^{-1}. As a cation, the NO_2^+ shows a strong tendency to bond to the TO. Then, A1-IM2 can be produced via transition state A1-TS1 with a barrier height of 41.6 kcal mol^{-1} with respect to the energy of A-IM1. A1-TS1 is formed by NO_2^+ directly attacking the target C1 atom of TO, as shown in Fig. 2. Consequently, the single bond of C(1)-H(2) is broken, and two single-bonds, H(2)-N(8) and C(1)-N(10), are formed simultaneously. Secondly, A1-IM2 converts to A-IM3, corresponding to an H-transfer process with the activation energy of 17.8 kcal mol^{-1}. In this process, H2 atom transfers from N8 to O12, so the bond length of N(8)-H(2) increases, whereas O12 and H2 atoms become close to together. As seen in path A2 in Fig. 1, A-IM3 can also be directly obtained via a concerned H-transfer transition state A2-TS1 with the barrier height of 45.7 kcal mol^{-1} in contrast to the energy of A-IM1. The subsequent processes were investigated separately in two different acidic systems. A-IM3 can be easily transformed into An-IM4 and As-IM4 in concentrated nitric acid and nitric-sulfuric acids, respectively. In both acids, the H abstraction from A-IM3 takes place barrierlessly, owing to larger electronegativity of O atom in NO_3^- and HSO_4^- groups (as shown in Fig. S2). Moreover, An-IM4 can isomerize into An-IM5 through An-TS3 with a barrier height of 38.8 kcal mol^{-1}. As shown in Fig. 2, An-TS3 has a very interesting geometrical structure, which is formed by breaking the O(16)-H(2) bond, and the H2 atom is simultaneously affected by three O atoms.

From above discussions, it is seen that the reaction steps via transition state A1-TS1 and A2-TS1 in path A1 and A2, respectively, are predicted as the rate-determining step. In A1-TS1, while H2 transfers to N8 atom, the influence of N8 atom to NO_2^+ decreased, so that the NO_2^+ can add to C1 atom. However, in A2-TS1, the transferring of H2 from C1 to O12 atom leads to the addition of NO_2^+ to C1 atom. In contrast with A1-TS1, possibly owing to the formation of a four-membered ring, A2-TS1 has higher activation barrier, implying that it is less likely to occur in path A.

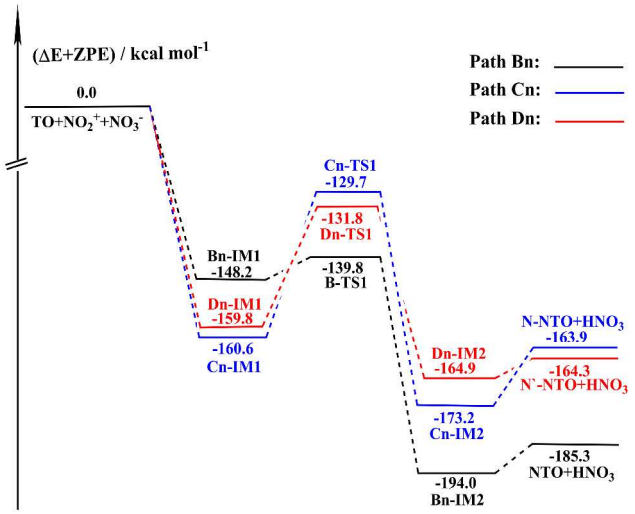

Fig. 3 Schematic energy diagram for potential energy surface of the NO_3^--induced nitration of TO predicted at the B3LYP/6-311++G(3df,3pd)//B3LYP/6-311G(d,p) level.

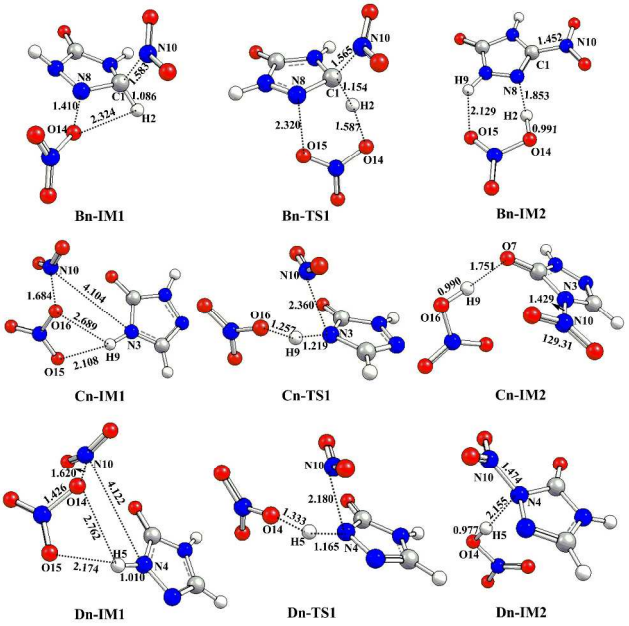

Fig. 4 Optimized geometries of species in the NO_3^--induced nitration calculated at the B3LYP/6-311G(d,p) level of theory (bond lengths are in angstrom).

3.1.2 NO_3^- induced nitration mechanism

We suggest that the nitration of TO in concentrated nitric acid may follow different mechanisms. In the presence of NO_3^-, the H2 on C1 is attracted by NO_3^- and leaves from C1, which makes the NO_2^+ attacking on C1 position of TO relatively easy during the reaction. In addition, the interaction of NO_3^- with different positions in the nitrogen heterocyclic molecule opens different nitration channels for NO_3^--induced reaction. In the present paper, three possible paths were taken into account. The paths, denoted as Bn, Cn, and Dn, respectively, as well as their schematic potential energy surfaces are shown in Fig. 3. The optimized geometries involved in NO_3^--induced nitration path Bn is shown in Fig. 4.

As seen in Fig. 3, the reactants first form complex Bn-IM2, which exists in the entrance of path Bn, and then produces the target product (NTO). The potential well depth of Bn-IM1 is 148.2 kcal mol^{-1} at the B3LYP/6-311++G(3df,3pd)//B3LYP/6-311G(d,p) level. Starting from Bn-IM1, Bn-IM2 can be obtained via the transition state Bn-TS1 with a barrier height of 8.4 kcal mol^{-1} relative to that of Bn-IM1. As shown in Fig. 4, the six-membered Bn-TS1 is mainly associated with the transferring of H2 from C1 to O14 atom and the simultaneous addition of NO_2^+ to C1 atom, leading to the formation of the intermediate Bn-IM2 in a concerted manner. In this process, the bond lengths of the C(1)-H(2), C(1)-N(10) and O(14)-H(2) change from 1.086, 1.583, and 2.324 Å to 2.962, 1.425, and 0.991 Å, respectively.

TO can be also transformed into 4-N-nitro-1,2,4-triazol-3-one (N-NTO) and 2-N-nitro-1,2,4-triazol-3-one (N`-NTO) by overcoming Cn-TS1 in path Cn and Dn-TS1 in path Dn, respectively. Similar to path Bn, the two paths (Cn and Dn) are also the NO_3^--induced nitration processes. The difference is that the latter two paths are hardly affected by the N8, owning to the relatively high negative charges of N3 and N4 atoms. The details of bond lengths are shown in Fig. 4. The activation barriers associated with path Cn and path Dn are calculated as 40.0 and 28.0 kcal mol^{-1}, respectively, at the B3LYP/6-311++G(3df,3pd)//B3LYP/6-311G(d,p) level.

As is clearly seen in Fig. 3, path Bn is the most favorable one for the NO_3^--induced nitration reaction among the above mentioned three paths. The possible reason is that Bn-TS1 is a six-membered transition state, in which the orbitals required for the bond dissociation and formation are deformed with relatively lower barriers.

It is of great interest whether the activation energy of path Bn is reduced by the induction effect of NO_3^- in concentrated nitric acid during the nitration process. Compared with the NO_2^+ direct nitration mechanism (in Fig. 1), the potential energy surfaces of the NO_3^--induced nitration mechanisms become straightforward and have lower barrier height, especially in path Bn (in Fig. 3). It is obvious that the nitration reaction is greatly enhanced by the participation of the NO_3^- and the resulted induction effect. From energetic point of view, the path Bn is much more favorable than others (path A, Cn and Dn), and therefore has high possibility to occur to produce the main product of NTO in the nitration of TO in concentrated nitric acid.

3.1.3 HSO_4^--induced nitration mechanism

We also found that the HSO_4^- can enhance the nitration of TO via a similar induction effect to that of NO_3^- when the nitric-sulfuric acids are used. Three possible paths are taken into account in the HSO_4^--induced nitration mechanism in nitric-sulfuric acids. The paths, which are denoted as Bs, Cs, and Ds, respectively, as well as their potential energy surfaces are shown in Fig. 5. The concerned bond lengths of all stationary points for the three paths are shown in Fig. 6.

Firstly, TO, NO_2^+ and HSO_4^- can form Bs-IM1 in path Bs, similar to that in path Bn. The activation energy associated with this step is calculated as 133.9 kcal mol^{-1} at the B3LYP/6-311++G(3df,3pd) level. Bs-IM1 is a six-membered ring structure, and the distance between N(8) and O(16) is 1.592 Å, as shown in Fig. 6. The formation of such structure may contribute great to

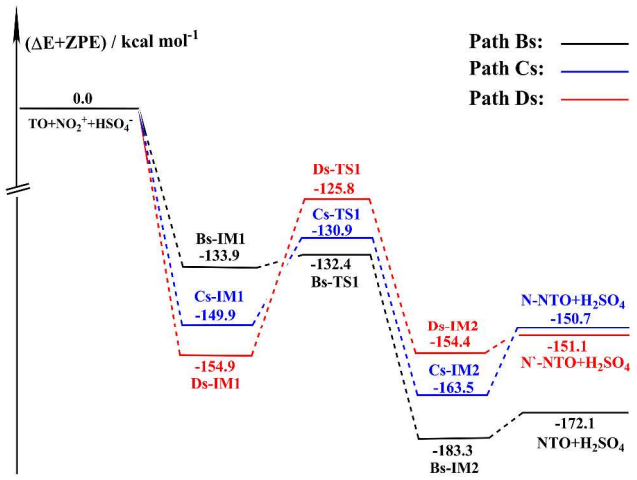

Fig. 5 Schematic energy diagram for potential energy surface of the HSO_4^--induced nitration of TO predicted at the B3LYP/6-311++G (3df,3pd)//B3LYP/6-311G(d,p) level.

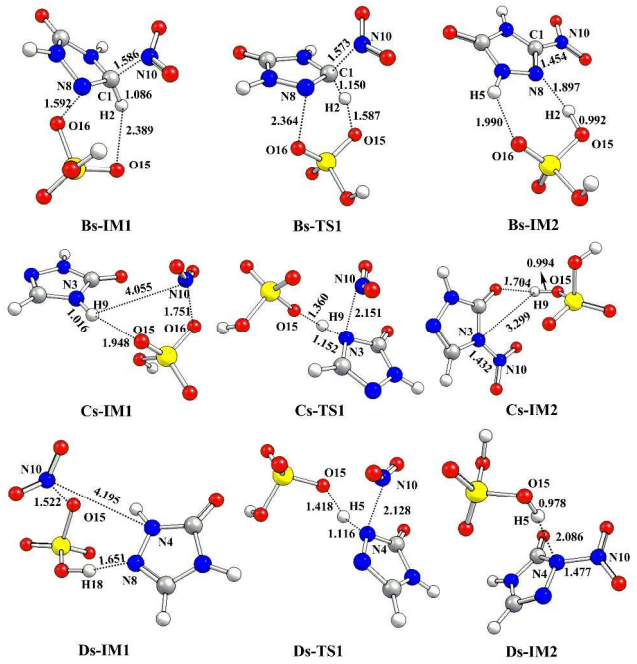

Fig. 6 Optimized geometries of species in the HSO_4^--induced nitration calculated at the B3LYP/6-311G(d,p) level (bond lengths are in angstrom).

the decrease of the attraction between N8 and NO_2^+, and promote the accessibility of NO_2^+ to C1 atom. As seen in Fig. 5, there is a reactive intermediate Bs-IM1 prior to the transition state Bs-TS1. Bs-TS1 has a very low barrier height of 1.5 kcal mol^{-1}, suggesting that the nitration of TO takes place almost spontaneously. Furthermore, energy of 47.5 kcal mol^{-1} (enthalpy changes) is released during the process from Bs-IM1 to Bs-IM2 at 298 K (as shown in Table 1). The results are exactly consistent with the experimental observations in the nitration of TO in nitric-sulfuric acids system[19]. In addition, similar to path Cn and Dn in the concentrated nitric acid system, paths Cs and Ds are HSO_4^--induced N-nitration processes of the nitrogen heterocyclic

molecules. As is shown in Fig. 5, Cs-IM2 (path Cs) and Ds-IM2 (path Ds) are obtained through the transition state of Cs-TS1 and Ds-TS1 with the barrier heights of 18.9 and 29.1 kcal mol^{-1}, respectively.

Compared with paths A, Cs and Ds, path Bs is the most favorable one for the nitration of TO to produce the main product of NTO in nitric-sulfuric acids due to its lowest barrier height (shown in Fig. 1 and Fig. 5). Moreover, path Bs is also more favorable than path Bn in view of the barrier height. In short, HSO_4^- can dramatically reduce the nitration barrier of TO with NO_2^+, and therefore remarkably promote the formation of NTO in nitric-sulfuric acids system.

3.1.4 Atomic charge of the pre-reactive intermediates

In order to further discern the reasons why the NO_3^--induced nitration (in concentrated nitric acid) and the HSO_4^--induced nitration (in nitric-sulfuric acids) are more likely to occur than the NO_2^+ direct nitration during the formation of NTO, the pre-reactive intermediates were investigated. The Mulliken atomic charges[49] of the pre-reactive intermediates in every rate-determining step were calculated at the B3LYP/6-311G(d,p) level. The calculated atomic charge of TO and some intermediates in the nitration of TO with NO_2^+ is shown in Table 2.

As shown in Table 2, N8 atom in TO has an atomic charge of -0.258 e, and can attract NO_2^+ to form A-IM1. While the formation of A-IM1 makes it difficult to form NTO. Fortunately, it is clearly seen that NO_3^- and HSO_4^- can effectively decrease the negative atomic charge of N8 in the corresponding intermediates. For example, from N8 in A-IM1, to that in Bn-IM1 and in Bs-IM1, the atomic charge of N8 is found to become more positive (from -0.226 to -0.131 and -0.133 e, respectively). Moreover, it is seen that NO_3^- and HSO_4^- can distinctly decrease the positive atomic charge of C1 in the corresponding intermediates. From C1 in A-IM1, to that in Bn-IM1 and in Bs-IM1, the atomic charge of C1 is found to decrease from 0.369 to 0.274 and 0.262 e, respectively. Simultaneously, the change of the atomic charge of N10 is found to be not as regular as that of N8 and C1. From A-IM1 to Bn-IM1, the atomic charge of N10 slightly increases from 0.475 to 0.481e. In view of the effective decrease of the negative atomic charge of N8, as well as the distinct decrease of the positive atomic charge of C1, it is inferred that the attraction between N10 and N8 as well as the repulsion between N10 and C1 may both decrease to a different extent. While from A-IM1 to Bs-IM1, the atomic charge of N10 is found to dramatically decrease from 0.475 to 0.236 e. It can also be inferred that the attraction between N10 and N8 as well as the repulsion between N10 and C1 may both obviously decrease. Owing to such factors, it is concluded that Bn-IM1 and Bs-IM1 are better candidates to produce NTO, especially does Bs-IM1.

As a result of above findings, the NO_3^--induced and HSO_4^--induced processes (path Bn and Bs) associated with the synthesis of NTO in concentrated nitric acid and nitric-sulfuric acids are much more favorable than path A due to their obviously positive effects on reducing the nitration barriers. Therefore, in view of the barrier height of 29.8 kcal mol^{-1} in the nitration of TO using HNO_3 as the nitration reagent calculated at the B3LYP/6-31G(d,p) level[21], and the results in the present paper, it is concluded that the nitration of TO in nitric-sulfuric acids is the most favorable one, which follows the path Bs in the HSO_4^--induced nitration mechanism.

Table 2 The calculated Mulliken atomic charges (e) of TO and some intermediates in the nitration of TO with NO_2^+ at the B3LYP/6-311G(d,p) level.

Species	C(1)	H(2)	N(3)	N(4)	H(5)	C(6)	O(7)	N(8)	H(9)	N(10)
TO	0.119	0.156	-0.392	-0.295	0.267	0.466	-0.307	-0.258	0.244	—
A-IM1	0.367	0.218	-0.373	-0.246	0.314	0.508	-0.218	-0.226	0.317	0.475
Bn-IM1	0.274	0.193	-0.397	-0.253	0.267	0.465	-0.315	-0.131	0.256	0.481
Bs-IM1	0.262	0.232	-0.399	-0.258	0.275	0.498	-0.303	-0.133	0.266	0.236

3.2 Kinetics for the nitration of TO

3.2.1 Effect of temperature on rate constants of the rate-determining step

For that the nitration of TO in concentrated nitric acid or nitric-sulfuric acids mostly occurs at relative low temperature ranges in experiments, the kinetics of the elementary reactions in every nitration path is investigated at temperature ranges of 225-400 K. The rate constants are calculated at different temperatures in the rate-determining step in nitration paths without and with NO_3^- /HSO_4^- by using the conventional TST, CVT and CVT with the SCT correction, respectively, at the B3LYP/6-311++G(3df,3pd)// B3LYP/6-311G(d,p) level. The relationships between the logarithm of TST, CVT, and CVT/SCT rate constants and temperature of path A1 are shown in Fig. S3. It is obvious that the SCT correction plays an important role for path A1 at the investigated temperature ranges (as shown in Fig. S3). The CVT/SCT rate constants for above mentioned paths are presented in Table 3.

It is clearly seen that the computed CVT/SCT rate constants in the rate-determining step in the NO_3^--induced path Bn (k'_{Bn}) are much larger than the corresponding values of the direct nitration path A (k'_{A1} and k'_{A2}) and the NO_3^--induced path Cn (k'_{Cn}), and Dn (k'_{Dn}), as shown in Table 3. It is indicated that the formation of NTO through the NO_3^--induced path Bn is the dominant way in the nitration of TO in concentrated nitric acid system. The small k'_{A1} and k'_{A2} imply that the direct nitration is unlike to occur at the investigated temperature ranges. Moreover, it is clear that k'_{Cn} and k'_{Dn} increase much faster than k'_{Bn} with the increase of temperature. Therefore, to suppress the side reactions and promote the selectivity of the targeted product of NTO, the nitration of TO in concentrated nitric acid should be carried out at relatively low temperature, which is in good agreement with the experimental observations[18].

The effect of temperature on every rate constant of rate-determining step for the nitration of TO in nitric-sulfuric acids is found to be similar to that in concentrated nitric acid system, as shown in Table 3. However, it is seen that the k'_{Bs} in HSO_4^--induced path is much larger than the k'_{Bn} in NO_3^--induced path, indicating that the nitration of TO in nitric-sulfuric acids is more favorable than that in concentrated nitric acid. Meanwhile, with the increase of temperature, k'_{Bs} increases much slower than k'_{Cs} and k'_{Ds}. Therefore, the nitration of TO in nitric-sulfuric acids system, prefers relatively low temperature in order to promote the selectivity of NTO, which is also consistent with the experimental observations[19].

Cite this: DOI: 10.1039/c0xx00000x

www.rsc.org/xxxxxx

ARTICLE TYPE

Table 3 The calculated rate constants ($cm^3 \cdot molecule^{-1} \cdot s^{-1}$) of the rate-determining step for the nitration of TO at temperature ranges of 255-400 K.

T/K	k'_{A1} [a]	k'_{A2}	k'_{Bn} [b]	k'_{Bs} [c]	k'_{Cn}	k'_{Cs}	k'_{Dn}	k'_{Ds}
255	1.82E-24	1.05E-26	5.09E+06	2.49E+13	1.29E-11	2.41E-02	3.43E-10	4.65E-11
265	4.19E-23	3.12E-25	8.42E+06	2.52E+13	9.94E-11	7.94E-02	2.21E-09	3.46E-10
270	1.84E-22	1.55E-24	1.07E+07	2.53E+13	2.61E-10	1.40E-01	5.32E-09	8.92E-10
273	4.37E-22	3.94E-24	1.23E+07	2.54E+13	4.57E-10	1.94E-01	8.89E-09	1.55E-09
276	1.02E-21	9.82E-24	1.40E+07	2.55E+13	7.92E-10	2.67E-01	1.47E-08	2.66E-09
280	3.04E-21	3.22E-23	1.67E+07	2.56E+13	1.62E-09	4.06E-01	2.81E-08	5.37E-09
285	1.15E-20	1.35E-22	2.07E+07	2.58E+13	3.84E-09	6.74E-01	6.19E-08	1.26E-08
295	1.43E-19	2.07E-21	3.11E+07	2.60E+13	1.99E-09	1.76E+00	2.77E-07	6.32E-08
300	4.73E-19	7.58E-21	3.77E+07	2.62E+13	4.34E-08	2.78E+00	5.64E-07	1.36E-07
305	1.51E-18	2.66E-20	4.54E+07	2.63E+13	9.22E-08	4.32E+00	1.12E-06	2.87E-07
310	4.62E-18	8.94E-20	5.43E+07	2.64E+13	1.92E-07	6.63E+00	2.19E-06	5.88E-07
315	1.37E-17	2.90E-19	6.47E+07	2.65E+13	3.89E-07	1.00E+01	4.16E-06	1.18E-06
320	3.92E-17	9.04E-19	7.66E+07	2.67E+13	7.72E-07	1.50E+01	7.78E-06	2.32E-06
325	1.09E-16	2.73E-18	9.03E+7	2.68E+13	1.50E-06	2.21E+01	1.43E-05	4.47E-06
330	2.91E-16	7.95E-18	1.06E+08	2.69E+13	2.86E-06	3.22E+01	2.57E-05	8.43E-06
335	7.60E-16	2.25E-17	1.24E+08	2.70E+13	5.35E-06	4.65E+01	4.54E-05	1.56E-05
340	1.93E-15	6.16E-17	1.44E+08	2.71E+13	9.83E-06	6.63E+01	7.89E-05	2.84E-05
350	1.14E-14	4.24E-16	1.91E+08	2.73E+13	3.15E-05	1.31E+02	2.28E-04	8.94E-05
360	6.15E-14	2.63E-15	2.51E+08	2.76E+13	9.44E-05	2.49E+02	6.19E-04	2.64E-04
370	3.02E-13	1.47E-14	3.25E+08	2.78E+13	2.67E-04	4.57E+02	1.60E-03	7.36E-04
380	1.37E-12	7.56E-14	4.14E+08	2.80E+13	7.16E-04	8.13E+02	3.91E-03	1.95E-03
400	2.22E-11	1.56E-12	6.50E+08	2.83E+13	4.44E-03	2.36E+03	2.06E-02	1.18E-02

[a] k'_{A1} and k'_{A2} denote the rate-determining step rate constant of path A1 and A2 for the NO_2^+ direct nitration in concentrated nitric acid or nitric-sulfuric acids, respectively. [b] k'_{Bn}, k'_{Cn} and k'_{Dn} denote the rate-determining step rate constant of path Bn, Cn and Dn for the NO_3^--induced nitration in concentrated nitric acid, respectively. [c] k'_{Bs}, k'_{Cs} and k'_{Ds} denote the rate-determining step rate constant of path Bs, Cs and Ds for the HSO_4^--induced nitration in nitric-sulfuric acids, respectively.

3.2.2 Effect of concentration on the nitration rate

Zbarsky et al.[20] found that the rate of the synthesis of NTO in nitric acid significantly depends on the concentration of the nitric acid used. In the present paper, the overall reaction rates of the direct nitration, the NO_3^--induced nitration, and the HSO_4^--induced nitration are investigated so as to explore the effects of concentrations of reactants on the nitration rate. When the nitration of TO follows the path A, the overall reaction rate in this direct nitration can be expressed as eqn. (3) as follows.

$$v_A = k_A[NO_2^+][TO] \quad (3)$$

While the nitration of TO is carried out in concentrated nitric acid and the overall reaction rate for the NO_3^--induced and HSO_4^--induced reactions can be expressed as eqn. (4) and (5), respectively.

$$v_{Bn} = k_{Bn}[NO_3^-][NO_2^+][TO] \quad (4)$$

$$v_{Bs} = k_{Bs}[HSO_4^-][NO_2^+][TO] \quad (5)$$

where k_{Bn} and k_{Bs} are the overall rate constants of the NO_3^--induced path Bn and HSO_4^--induced path Bs, respectively. The relative rate in each nitration system is defined as eqn. (6) and (7) as follows.

$$\frac{v_{Bn}}{v_A} = \frac{k_{Bn}}{k_A}\frac{[NO_3^-][NO_2^+][TO]}{[NO_2^+][TO]} = \frac{k_{Bn}}{k_A}[NO_3^-] \quad (6)$$

as well as

$$\frac{v_{Bs}}{v_A} = \frac{k_{Bs}}{k_A}\frac{[HSO_4^-][NO_2^+][TO]}{[NO_2^+][TO]} = \frac{k_{Bs}}{k_A}[HSO_4^-] \quad (7)$$

It is clearly seen in eqn. (6) and (7) that both the relative rates depend on the corresponding rate constants. More importantly, the concentrations of NO_3^- and HSO_4^- impact significantly and positively on the nitration rates in the corresponding nitration systems. In this case, it is inferred that relatively dilute acids may be favorable to the induction effects of NO_3^-/HSO_4^-, since NO_3^-/HSO_4^- is apt to be easily released in dilute acids. While a higher acid concentration may definitely benefit an easier formation of NO_2^+, benefiting the nitration of TO. Therefore, the concentrations of both HNO_3 and H_2SO_4 in both nitration systems should be well controlled as the favorable condition to produce

NO_2^+ and NO_3^-/HSO_4^- differs in the concentrations of the corresponding acids.

4. Conclusions

Three nitration mechanisms of TO with NO_2^+ in both concentrated nitric acid and nitric-sulfuric acids were investigated and proposed in the present paper at the B3LYP/6-311G(d,p) level, including the NO_2^+ direct nitration (path An, As), NO_3^--induced nitration (paths Bn-Dn), and HSO_4^--induced nitration (paths Bs-Ds), respectively. It is clear seen that the NO_3^--induced and HSO_4^--induced nitration paths are more favorable to occur than the NO_2^+ direct nitration path, attributing to the proclaimed induction effects of NO_3^- and HSO_4^- and the resulted significant decrease of the activation energy during the nitration processes. Additionally, the decrease of energy barrier in path Bs is further explained by using the atomic charge calculation of pre-reactive intermediates (A-IM1, Bn-IM1, and Bs-IM1) for the synthesis of NTO.

The nitration kinetics of TO in both concentrated nitric acid and nitric-sulfuric acids were also investigated. The effects of temperature on the rate constants of rate-determining steps were explored. The calculated results of CVT/SCT rate constants show that NO_3^- and HSO_4^- effectively accelerate the nitration of TO with NO_2^+, indicating that NO_3^-/HSO_4^- acts as a catalyst during the nitration process. It is also concluded that the nitration reaction of TO with NO_2^+ to form NTO in concentrated nitric acid and nitric-sulfuric acids are more favourable at low temperatures. And the concentrations of NO_3^- and/or HSO_4^- significantly impact on the nitration rates of the corresponding nitration systems. Therefore, in view of the fact that a higher acid concentration may benefit an easier formation of NO_2^+, the concentrations of both HNO_3 and H_2SO_4 should be well controlled since the favourable condition to produce NO_2^+ and NO_3^-/HSO_4^- differs in the concentrations of the corresponding acids.

The catalytic effects of the nitric acid and sulfuric acid are thought to be embodied in not only the acceleration to the formation of NO_2^+, but also the proclaimed induction effects of NO_3^- and/or HSO_4^- during the nitration processes. We believe that it is such catalytic effects of the nitric acid and sulfuric acid, especially the induction effects of NO_3^- and HSO_4^- that make the nitration mechanism of TO differ in that of the aromatics. It is expected that the present study may provide a theoretical basis to the research and engineering amplification of the preparation of NTO as well as other energetic materials.

Acknowledgment

The authors gratefully acknowledge the financial support of the National Natural Science Foundation of China (21306111, 21327011), Shaanxi Innovative Team of Key Science and Technology (2012KCT-21, 2013KCT-17), Natural Science Foundation of Shaanxi Province (2014JM2034), and the Fundamental Research Funds for the Central Universities (GK201401001, GK201402050).

Notes and references

[a] *Key Laboratory of Applied Surface and Colloid Chemistry (MOE) and School of Chemistry & Chemical Engineering, Shaanxi Normal University, Xi'an, 710119, China. Fax: +86 29 8153 0727; Tel: +86 29 8153 0803; E-mail: jgchen@snnu.edu.cn*

[b] *Research Center for Eco-Environmental Science, Chinese Academy of Sciences, Beijing,10085, China*

[c] *Department of Catalytic Technology, Institute of Xi'an Modern Chemistry, Xi'an, 710065, China. Fax: +86 29 8829 1213; Tel: +86 29 8829 1213; E-mail: lujian204@gmail.com*

† Electronic Supplementary Information (ESI) available: Schematic diagram for the attraction of NO_2^+ by TO molecule during the nitration process is shown in Fig. S1. The potential energy surface scan of O(16)-H(2) in An-IM4, and the potential energy surface scan of O(15)-H(2) in As-IM4, calculated at the B3LYP/6-311G(d,p) level, and are shown in Fig. S2 (a) and (b). T The calculated rate constants of the rate-determining step of path A1 via TST, CVT and CVT/SCT within temperature ranges of 225-400 K are shown in Fig. S3. See DOI: 10.1039/b000000x/

1 K. Y. Lee and R. Gilardi. Mater. *Res. Soc. Symp. Proc.,* 1993, **296**, 237-242.
2 E. F. Rothgery, D. E. Audette, R. C. Wedlich and D. A. Csejka, *Thermochim. Acta,* 1991, **185**, 235-243.
3 N. B. Bolotina, E. A. Zhurova and A. A. Pinkerton, *J. Appl. Crystallogr.,* 2003, **36**, 280-285.
4 B. C. Beard and J. Sharma, *J. Energ. Mater.,* 1993, **11**, 325-343.
5 K. Y. Lee, L. B. Chapman and M. D. Coburn, *J. Energetic Mat.,* 1987, **5**, 27-33.
6 Y. Xie, R. Z. Hu, X. Y. Wang, X. Y. Fu and C. H. Zhu, *Thermochim. Acta.,* 1991, **189**, 283-296.
7 G. K. Williams and T. B. Brill, *J. Phys. Chem.,* 1995, **99**, 12536-12539.
8 J. C. Oxley, J. L. Smith, K. E. Yeager, E. Rogers and X. X. Dong, *Mater. Res. Soc. Symp. Proc.*, 1996, **418**, 135-142.
9 T. R. Botcher, D. J. Beardall, C. A. Wight, L. Fan and T. J. Burkey, *J. Phys. Chem.,* 1996, **100**, 8802-8806.
10 D. F. McMillen, D. C. Erlich, C. He, C. H. Becker, and D. A. Shockey, *Combust. Flame.,* 1997, **111**, 133-160.
11 N. L. Garland, H. D. Ladouceur and H. H. Nelson, *J. Phys. Chem. A.,* 1997, **101**, 8508-8512.
12 N. J. Harris and K. Lammertsma, *J. Am. Chem. Soc.,* 1996, **118**, 8048-8055.
13 C. Meredith, T. R. Russell, R. C. Mowrey and J. R. McDonald, *J. Phys. Chem. A,* 1998, **102**, 471-477.
14 Y. M. Wang, C. Chen and S. T. Lin, *J. Mol. Struct. (THEOCHEM),* 1999, **460**, 79-102.
15 D. C. Sorescu and D. L. Thompson, *J. Phys. Chem. B,* 1997, **101**, 3605-3613.
16 Y. Kohno, O. Takahashi and k. Saito, *Phys. Chem. Chem. Phys.,* 2001, **3**, 2742-2746.
17 W. L. Yim and Z. F. Liu, *J. Am. Chem. Soc.,* 2001, **123**, 2243-2250.
18 V. F. Zhilin and V. L.Zbarsky, *Chimicheskaya technologiya,* 2001, **5**, 6.
19 H. S. Kim, E. M. Goh and B. S. Park, *U.S. Patent 6583293,* 2003, Agency for Defense Development of Korean Republic.
20 V. L. Zbarsky, N. V Yudin, *Propellants, Explos., Pyrotech.,* 2005, **30**, 298-302.
21 K. F. Cheng, M. H. Liu and P. H. Yang, *Int. J. Quantum Chem.,* 2012, **112**, 703-712.
22 T. M. Klapoetke and J. Stierstorfer, *Helv. Chim. Acta.,* 2007, **90**, 2132-2150.
23 F. Cacace, M. Attina, G. De Petries and M. Speranza, *J. Am. Chem. Soc.,* 1990, **112**, 1014-1018.
24 E. L. Blackall and E. D. Hughes, *Nature,* 1952, **170**, 972-973.
25 E. D. Hughes, C. Ingold and R. B. Pearson, *J. Chem. Soc.,* 1958, 4357-4365.
26 E. L. Blackall, E. D. Hughes and C. Ingold, *J. Chem. Soc.,* 1958, 4366-4374.
27 N. C. Marziano, A. Tomasin, C. Tortato and J. M. Zaldivar, *Journal of the Chemical Society, Perkin Transactions 2: Physical Organic Chemistry,* 1998, (9), 1973-1982.
28 A. Swinarski and G. Bialozynski, *Roczniki Chemii.,* 1959, **33**, 907-918.

29 E. K. Kim, T. M. Bockman and J. K. Kochi, *J. Am. Chem. Soc.,* 1993, **115**, 3091-3104.

30 M. Liljenberg, T. Brinck, B. Herschend, T. Rein, G. Rockwell and M. Svensson, *J. Org. Chem.,* 2010, **75**, 4696-4705.

31 M. Haouas, S. Bernasconi, A. Kogelbauerb and R. Prins, *Phys. Chem. Chem. Phys.,* 2001, **3**, 5067-5075.

32 Z. H. Zhen and Y. R. Mo, *J. Chem. Theory Comput.,* 2013, **9**, 4428-4435.

33 A. Arrieta and F. P. Cossio, *J. Mol. Struct.: THEOCHEM,* 2007, **811**(1-3), 19-26.

34 This will be presented elsewhere.

35 Gaussian 09, Revision B.01, M. J. Frisch, G. W. Trucks, H. B. Schlegel, G. E. Scuseria, M. A. Robb, J. R. Cheeseman, G. Scalmani, V. Barone, B. Mennucci, G. A. Petersson, H. Nakatsuji, M. Caricato, X. Li, H. P. Hratchian, A. F. Izmaylov, J. Bloino, G. Zheng, J. L. Sonnenberg, M. Hada, M. Ehara, K. Toyota, R. Fukuda, J. Hasegawa, M. Ishida, T. Nakajima, Y. Honda, O. Kitao, H. Nakai, T. Vreven, J. A. Montgomery Jr., J. E. Peralta, F. Ogliaro, M. Bearpark, J. J. Heyd, E. Brothers, K. N. Kudin, V. N. Staroverov, T. Keith, R. Kobayashi, J. Normand, K. Raghavachari, A. Rendell, J. C. Burant, S. S. Iyengar, J. Tomasi, M. Cossi, N. Rega, J. M. Millam, M. Klene, J. E. Knox, J. B. Cross, V. Bakken, C. Adamo, J. Jaramillo, R. Gomperts, R. E. Stratmann, O. Yazyev, A. J. Austin, R. Cammi, C. Pomelli, J. W. Ochterski, R. L. Martin, K. Morokuma, V. G. Zakrzewski, G. A. Voth, P. Salvador, J. J. Dannenberg, S. Dapprich, A. D. Daniels, O. Farkas, J. B. Foresman, J. V. Ortiz, J. Cioslowski, D. J. Fox, *Gaussian, Inc.*, Wallingford, CT, 2010.

36 C. Lee, W. T. Yang and R. G. Parr, *Phys. Rev. B,* 1988, **37**, 785-789.

37 A. D. McLean and G. S. Chandler, *J. Chem. Phys.,* 1980, **72**, 5639-5648.

38 L. T. Chen, H. M. Xiao, J. J. Xiao and X. D. Gong, *J. Phys. Chem. A*, 2003, **107**, 11440-11444.

39 L. L. T. Chen, H. M. Xiao and J. J. Xiao, *J. Phys. Org. Chem.* 2005; **18**, 62-68.

40 A. L. X. Jin, W. L. Wang, D. D. Hu and S. T. Min, *J. Chem. Phys. B,* 2013, **117**, 3−12.

41 C. Gonzales and H. B Schlegel, *J. Chem. Phys.,* 1989, **90**, 2154-2161.

42 B. C. Garrett and D. G. Truhlar, *J. Chem. Phys.,* 1979, **70**, 1593-1598.

43 B. C. Garrett and D. G. Truhlar, *J. Am. Chem. Soc.,* 1979, **101**, 4534-4548.

44 C. GarrettB, D. G. Truhlar, R. S. Grev and A. W. Magnuson, *J. Phys. Chem.* 1980, **84**,1730-1748.

45 D. H. Lu, T. N. Truong, V. S. Melissas, G. C. Lynch, Y. P. Liu, B. C. Garrett, R. Steckler, A. D. Isaacson, S. N. Rai, G. C. Hancock, J. G. Lauderdale, T. Joseph and Truhlar D. G. *Comput. Phys. Commun.,* 1992, **71**, 235-262.

46 Y. P. Liu, T. N. Lynch, T. N. Truong, D. H. Lu, D. G. Truhlar and B. C. Garret, *J. Am. Chem. Soc.,* 1993, **115**, 2408-2415.

47 S. W. Zhang and T. N. Truong, *VKLab,Version 1.0*, University of Utah:Salt Lake City, 2001.

48 T. J. Lee and J. E. Rice, *J. Phys. Chem.,* 1992, **96**, 650-657.

49 R. S. Mulliken, *J. Chem. Phys.*, 1955, **23**, 1833-1840.